Aerospace Science and Technology 112 (2021) 106618

Contents lists available at ScienceDirect

Aerospace Science and Technology

www.elsevier.com/locate/aescte

Assessment of dynamic pairwise wake vortex separations for approach and landing at Vienna airport

Frank Holzäpfel [a,*], Lukas Strauss [b], Carsten Schwarz [c]

[a] Institut für Physik der Atmosphäre, Deutsches Zentrum für Luft- und Raumfahrt, 82234 Oberpfaffenhofen, Germany
[b] MeteoServe Wetterdienst GmbH / Austro Control GmbH, 1220 Vienna, Austria
[c] Institut für Flugsystemtechnik, Deutsches Zentrum für Luft- und Raumfahrt, 38108 Braunschweig, Germany

ARTICLE INFO

Article history:
Received 23 July 2020
Received in revised form 8 January 2021
Accepted 22 February 2021
Available online 1 March 2021
Communicated by Euan Mcgookin

Keywords:
Wake vortices
Wake vortex advisory system
Approach and landing
Pairwise dynamic separations
Safety assessment

ABSTRACT

The Wake Vortex Prediction System WSVS (WirbelSchleppenVorhersageSystem) has been developed to tactically increase airport capacity by employing dynamically adjusted aircraft separations for approach and landing without compromising safety. For this purpose, the WSVS considers the involved aircraft type pairing, the prevailing weather conditions, and the resulting wake vortex behavior. A Monte Carlo simulation study demonstrates that the WSVS is well adjusted to a reasonable level of safety. The simulation study evaluates the probability that wake vortices still linger within defined radii around the follower aircraft and compares this probability to measurement data collected at five major international airports. The potential of the WSVS to optimize aircraft separations is assessed by employing twelve months of traffic and weather prediction data collected at Vienna International Airport. Analyses of the separation reduction potential are established and compared to current regulations. Dependencies on prevailing headwind and crosswind conditions are discussed in terms of individual wake vortex behavior and statistical distributions of wake turbulence separations. The results indicate that substantial potential for safely reduced aircraft separations exists mainly under sufficiently strong crosswind conditions for any aircraft type combination requiring wake vortex separation minima.

1. Introduction

Aircraft trailing vortices, generated as an unavoidable consequence of lift, pose a potential risk to following aircraft. The separation standards between consecutive aircraft limit the capacity of congested airports in a rapidly growing aeronautical environment [1]. The most likely economic scenario for the future European airport demand indicates that there will be around 1.5 million unaccommodated flights in 2040, constituting approximately 8% of the expected demand [2]. Such a lack of capacity could mean 160 million passengers would not be able to travel with a potential economic loss of around € 88 billion to the European economy. To date there is no estimate available to what extent this outlook may have to be adjusted in view of the COVID-19 crisis.

Comprehensive research has been conducted aiming at a better understanding of wake vortex behavior, the translation of this knowledge into fast-time prediction models, and the design of complete wake vortex advisory systems conceived to increase airport capacity [1]. During approach and landing the roll-up of the vorticity [3] shed from the wings in high-lift configuration is being complicated by the merging process of the heterogeneous vortex system forming in the wake near field [4] and its interaction with the exhaust jets [5]. The subsequent wake vortex behavior in the atmosphere is controlled by the prevailing wind, wind shear, thermal stratification, and turbulence [6], [7].

In ground proximity, vortex descent, rebound and decay characteristics are controlled by the interaction of the vortices with the secondary vorticity detaching from the ground [8], [9], [10]. Crosswind shear is leading to asymmetrical rebound characteristics, where the luff vortex that may linger in the flight corridor features slower decay rates [8], [9]. Very close to the ground the interaction of the flap-tip and wingtip vortices with the vorticity layer generated at the ground surface add additional complexity [11], [12]. To adjust aircraft separations this complexity can be disregarded because during this flight phase so-called end effects

* Corresponding author.
E-mail addresses: frank.holzaepfel@dlr.de (F. Holzäpfel), lukas.strauss@meteoserve.at (L. Strauss), carsten.schwarz@dlr.de (C. Schwarz).

https://doi.org/10.1016/j.ast.2021.106618

Nomenclature

b	vortex separation
N	Brunt-Väisäla frequency
r	radial distance
RCR	roll control ratio
t	time coordinate, also vortex time scale
t_{sep}	separation time between landing aircraft
T	temperature
T_{pot}	potential temperature
TAS	true airspeed
TKE	turbulence kinetic energy
u	longitudinal wind component, positive in flight direction
v	crosswind component
w	wake vortex descent speed
q	turbulence velocity
x	coordinate in flight direction
x_{sep}	separation distance between landing aircraft
y	coordinate in lateral direction
z	coordinate in vertical direction
ϵ	turbulence energy dissipation rate
Γ	vortex circulation
σ	standard deviation

Superscripts

*	normalized quantity

Subscripts

0	initial value

Abbreviations

a/c	aircraft
AIAA	American Institute of Aeronautics and Astronautics
APA	AVOSS prediction algorithm
BADA	Base of Aircraft Data
CAA	Civil Aviation Authority
DLR	Deutsches Zentrum für Luft- und Raumfahrt
DVM	deterministic wake vortex model
EASA	European Union Aviation Safety Agency
ECMWF	European Centre for Medium-Range Weather Forecasts
EU	European Union
FAA	Federal Aviation Administration
FAF	final approach fix
H, HVY	Heavy ICAO wake turbulence category
ICAO	International Civil Aviation Organization
IFS	Integrated Forecasting System
J	Super ICAO wake turbulence category
L	Light ICAO wake turbulence category
lidar	light detection and ranging
M, MED	Medium ICAO wake turbulence category
MLW	maximum landing weight
NASA	National Aeronautics and Space Administration
P2P	probabilistic two-phase wake vortex model
RECAT	wake turbulence re-categorization
SHAPe	simplified hazard area prediction
TCDS	type certificate data sheet
TDAWP	TASS driven algorithms for wake prediction
TDZ	touchdown zone
UTC	universal time coordinate
WSVBS	WirbelSchleppenVorhersage- und -BeobachtungsSystem (wake vortex prediction and monitoring system)
WSVS	WirbelSchleppenVorhersageSystem (wake vortex prediction system)

propagating from the touchdown zone accelerate wake vortex decay substantially [13], [14]. All those parameters and effects control the potential of suitably reduced aircraft separations and the resulting airport capacity [15], [16], [17].

Over the years a number of fast-time wake vortex prediction models have been suggested that are using physics-based empirical parameterizations to mimic vortex transport and decay. The first fast-time model suggested by Greene in 1986 [18] served as inspiring example for subsequent model developments including the model of Kantha [19], APA [20], P2P [21], TDAWP [22], and DVM [23].

A few years ago, the International Civil Aviation Organization (ICAO) initiated a process for the optimization of wake turbulence separations termed RECAT. RECAT phase I, which is the classification into six categories considering the weight, approach speed, wing characteristics and the rolling moment exerted on following aircraft, has been implemented at selected airports in the US [24] and Europe [25]. RECAT phase II consists of a static separation matrix of distance and time for individual aircraft types (pairwise separations) based upon similar metrics as RECAT I. The long-term goal of the RECAT initiative (phase III) foresees dynamic pairwise separations that consider the aircraft type pairing and the effects of the environmental conditions on wake vortex behavior. Surveys on further procedural modifications meant to increase airport capacity and on wake-vortex advisory systems are available in Refs. [1] and [26].

The Wake Vortex Prediction and Monitoring System WSVBS (Wirbelschleppenvorhersage- und -beobachtungssystem) has been developed to tactically increase airport capacity by employing dynamically adjusted aircraft separations for approach and landing dependent on weather conditions and the resulting wake vortex behavior without compromising safety [27], [28], [29]. This study considers only the predictive part of the WSVBS system, whereas the monitoring aspects are excluded. Therefore, in this paper the advisory system is simply called Wake Vortex Prediction System (WirbelSchleppenVorhersageSystem) WSVS.

The WSVS combines several probabilistic elements and conservative assumptions in order to make its predictions safe. However, it is not obvious how the degree of safety resulting from the combination of these conservative elements could be estimated. In order to demonstrate that the WSVS is well adjusted to a reasonable level of safety, the probabilities that wake vortices still linger within defined radii around the follower aircraft at the dynamically adjusted aircraft separations is estimated via Monte Carlo simulation. The resulting probabilities are compared to measurement data collected by NASA and DLR at 5 major international airports.

Next, this paper assesses the potential of the WSVS to optimize aircraft separations employing data of 106,293 individual aircraft pairings approaching Vienna International Airport during one complete year. Traffic data comprising aircraft types and flight speeds along selected positions of the approach are retrieved from the Mode-S protocol. Meteorological data comprising vertical profiles of horizontal wind, potential temperature, and air density are taken from weather predictions of the IFS of the ECMWF. Turbulence kinetic energy is derived from a Richardson-number-based approach.

The analysis covers statistics of the achievable aircraft separation reduction potential compared to the separation matrices of ICAO and RECAT-EU. The correlation between the vertical profiles of headwind and crosswind and the separation reduction potential

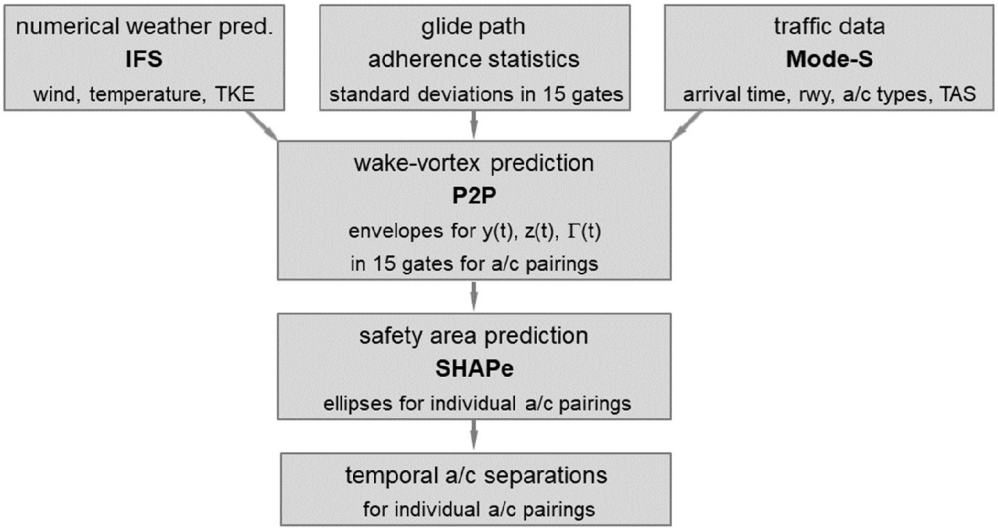

Fig. 1. Flowchart detailing the components of the wake vortex prediction system WSVS.

is elaborated. Exemplary case studies on landing rates, meteorological conditions, and spatial and temporal aircraft separations as actually flown and as predicted by the WSVS are introduced as examples for possible developments throughout a day. In order to better understand the mechanisms controlling the temporal aircraft separations in headwind and crosswind situations, the developments of wake vortex parameters and safety areas in individual WSVS prediction planes are analyzed for selected cases.

The results indicate that substantial potential for reduced separations emerges for any aircraft type combination requiring wake vortex separations under strong crosswind conditions. The WSVS predictions for strong headwinds reveal only a modest potential of separation reduction. However, the discussed headwind effects provide interesting insights with respect to time-based procedures for arrivals, which will have to be implemented at large European airports in the next 5 to 10 years.

A precursor version of this article based on 78,119 approaches and landings covering 9 months of arrivals has been presented at the AIAA Aviation 2019 Forum [30]. In this previous version, the period July to September 2018 could not yet be integrated due to missing data of aircraft types, which have now been reconstructed.

2. The Wake Vortex Prediction System WSVS

Initially, the Wake Vortex Prediction and Monitoring System WSVBS has been developed to tactically increase airport capacity for approaches to the closely-spaced parallel runway system of Frankfurt airport [27], [28]. Later the WSVBS has been extended to predict dynamic pairwise separations for landings on single runways [29]. Demonstration campaigns at the airports Frankfurt and Munich substantiated that the WSVBS predictions were safe for all of the about 2000 landings where the wake vortex behavior was measured by lidar. In this paper only the predictive part of the WSVBS system is considered and the monitoring aspects are excluded; therefore, we will refer to the Wake Vortex Prediction System WSVS in the remainder of this paper. The complete WSVBS employs wake vortex measurements to monitor the reliability of the WSVS. In the following, the main components of the WSVS are briefly introduced and a few new developments are sketched in some more detail.

Fig. 1 delineates the components of the WSVS and their interplay as they are applied to the data base available from Vienna airport. The meteorological conditions are taken from operational predictions of the IFS of the ECMWF with a model output interval of three hours. A single vertical profile of wind speed, potential temperature and air density is used to describe the meteorological conditions in all four approach corridors associated with the two airport runways. TKE is derived from thermal stability and wind gradients employing a Richardson number-based approach [31], [32]. The TKE is translated into turbulence dissipation rate according to the approximate formula provided by Ref. [34].

The considered arrival traffic consists of 106,293 approaches and landings on the runways 11/29 and 16/34 during the months November 2017 to October 2018. The aircraft data base of the WSVS contains 94 different aircraft types covering more than 95% of the arrivals at Vienna Airport. Within that traffic mix 94% correspond to medium weight class aircraft and only 6% are heavies. From Mode-S data protocols aircraft types and true airspeeds within the prediction planes of the WSVS are retrieved. Mode-S is a secondary surveillance radar process that allows selective interrogation of aircraft employing ground-based interrogators and airborne transponders [33]. The weights of the approaching aircraft are adjusted to 85% of the MLW. Measurements at the airports Memphis and Dallas Fort Worth demonstrate that the landing weight on average amounts to 85% of the MLW [35] and other sources confirm this result [36]. Wing spans are gathered from the BADA data base [37] and MLWs mainly from type certificate data sheets from EASA, FAA, and CAA and airplane characteristics for airport planning from Airbus and Boeing.

The WSVS concept requires that all aircraft are established on the glide slope at the final approach fix which is considered 11 nm before the touchdown zone for this study. A merger of fits of glide path adherence statistics from different sources collected at the airports Frankfurt, St. Louis, Atlanta, and Chicago is used to define the dimensions of the flight corridors in terms of standard deviations from the nominal glide paths [29]. Wake vortex evolution is predicted within 15 gates along the final approach (see Table 1). In ground proximity the gate separation of 1 nm is first reduced to 1/3 nm and then to 1/6 nm to properly resolve the interaction of wake vortices with the ground. The WSVS prediction planes are transported by the prevailing headwind respectively tailwind allowing for a realistic modeling of wake vortex behavior in ground proximity. This constitutes an important aspect for the simulation of landings, because wake vortex encounters at low altitudes appear more frequently in tailwind situations [38].

Based on the meteorological and traffic input data the Probabilistic Two-Phase wake-vortex model (P2P) predicts upper and lower bounds for position and strength of the vortices. The ba-

Table 1
Initial gate (prediction plane) center positions along glide path in geodetic coordinates (origin in touchdown zone).

Gate No.	x_{gate} [nm]	x_{gate} [m]	z_{gate} [m]
1	−11	−20372	−1077
2	−10	−18520	−979
3	−9	−16668	−880
4	−8	−14816	−781
5	−7	−12964	−683
6	−6	−11112	−584
7	−5	−9260	−486
8	−4	−7408	−387
9	−3	−5556	−289
10	−2	−3704	−191
11	−1.5	−2778	−142
12	−1	−1852	−94
13	−2/3	−1235	−61
14	−1/3	−617	−29
15	−1/6	−309	−13

sic P2P model design as well as some applications, assessments and further developments are reported in Refs. [21], [39], [40], and [8]. P2P considers all effects of the leading-order impact parameters: aircraft parameters (wing span, weight, velocity, and attitude angles), wind (crosswind and headwind components), wind shear, turbulence, thermal stratification, and ground proximity [7]. P2P has been validated against in-ground effect and out-of-ground effect measurement data of four US and nine European field measurement campaigns comprising about 15,000 individual cases.

The bounds predicted by P2P are expanded by the safety area around a vortex that must be avoided by follower aircraft for safe and undisturbed flight employing the simplified hazard area prediction model SHAPe. The simplified hazard area concept [41], [42] assumes that, for encounters during approach and landing, the vortex-induced rolling moment constitutes the dominant effect and can be used to define a safety area representing the entire aircraft reaction. Then encounter severity can be characterized by a single parameter, the roll control ratio, which relates the wake vortex induced rolling moment to the maximum available roll control power. Following full flight simulator investigations as well as real flight tests *RCR* is adjusted to 0.2 (Ref. [43]).

In every gate listed in Table 1 several ellipses are defined (see Fig. 2) representing the approach corridor (green), the probabilistic vortex corridor (blue), and the safety area (red). The vortex corridor moves with the predicted vortex location and it increases in size with the increasing uncertainty allowances while the safety corridor shrinks with time as the vortex circulation decays. The respective sums of the vertical and horizontal probabilistic allowances of the components approach corridor, wake vortex location, and safety area define the dimensions of the resulting red safety ellipse. The instant when all the resulting safety ellipses along the glideslope do not overlap anymore with the elliptical approach corridor defines the temporal minimum wake-vortex separation between an individual aircraft pairing [27], [29]. For operational purposes, the maximum of three time thresholds, the WSVS separation, the minimum radar separation, and the runway occupancy time, would then constitute the applicable separation. In this study, however, these additional criteria are neglected to allow an independent consideration and comparison of those three time thresholds. The maximum prediction time of the WSVS is adjusted to 180 s.

3. How conservative are the WSVS predictions compared to current practice?

The WSVS combines several conservative assumptions and probabilistic elements in order to make its predictions safe. One key element of its current setup is that the WSVS adds to the

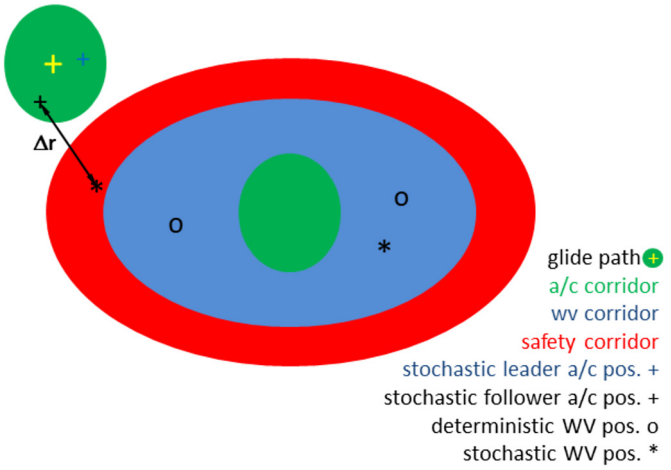

Fig. 2. Scheme illustrating the elliptical areas used for the WSVS predictions in every gate. Black symbols denote elements of Monte-Carlo simulation described in section 3. (For interpretation of the colors in the figure(s), the reader is referred to the web version of this article.)

one-σ (68.3%) semi-axes of the aircraft approach corridor one-σ-allowances resulting from the variability of wake vortex behavior (P2P) and further adds finite safety separation distances (SHAPe) (see Fig. 2). The instant of time when these areas, each consisting of three ellipses, do not overlap anymore with the aircraft corridor in all 15 gates determines the WSVS aircraft separations. However, neither the probability that the wake vortices including their individual safety area reside within the predicted elliptical total safety area, nor the probability that the wake vortices may still reside in the flight corridor or actually come close to a follower aircraft are known. The latter probability is the most relevant one for the degree of safety of the advisory system. So, the probability that wake vortices still linger within a defined radius around the follower aircraft is estimated in this section and compared to measurement data collected by NASA and DLR at five major international airports.

More precisely, Monte Carlo simulation is employed in order to establish statistics of the distances between a landing aircraft and the closest wake vortex generated by a leading aircraft at the separation time suggested by the WSVS. These distances are compared to those found within the analysis of lidar measurements and aircraft data described in Ref. [44]. The lidar study employs data of 8056 landings collected at the airports Dallas, Denver, Frankfurt, Memphis, and Munich. During the Memphis 2013 campaign RECAT separations [24] were applied while during the other campaigns ICAO separations [45] were applicable. The analysis of the lidar observations reveals that, in at least 1.5% (3.7%) of the landings in which the measured vortices were generated in an altitude of about 50 m, the luff vortex remains within a distance of 25 m (50 m) to the follower aircraft within a temporal buffer of ±10 s of flyby. This finding is considered as a reference for the current safety assessment. For comparison the Frankfurt wake vortex warning system considered a 30 m distance between fuselage and wake vortices as a critical gap differentiating between acceptable and critical encounters [46].

The lidar study considers only wake vortices with circulation strengths above 50% of their initial value, because most vortices with a circulation less than half of their initial circulation cannot be tracked anymore. As a consequence, many encounters with less coherent vortices are not included in the above stated encounter percentages and the real encounter rates will be higher. Note that here the term encounter is used for situations with distances of up to 50 m between fuselage and vortex center. Hence, the term

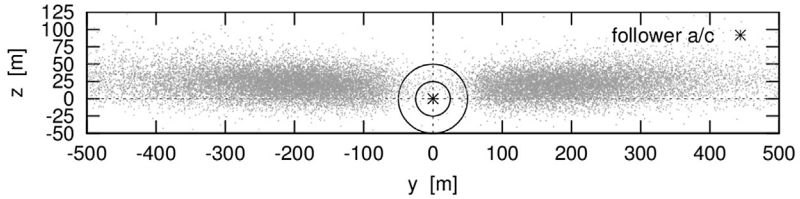

Fig. 3. Scatter plot of vortex positions relative to follower aircraft at predicted WSVS aircraft separation times. Circles represent 25 m and 50 m distances between follower aircraft and wake vortices evaluated in this study.

encounter is also used for cases without any vortex effect on the passing aircraft.

In the Monte Carlo simulation we only exclude wake vortices with circulation values below 50 m^2/s. Below this value the evaluation of the circulation of the vortices is usually not possible anymore due to a loss of coherence of the vortex structure. Also, for circulation values below 50 m^2/s the safety areas to be avoided according to the SHAPe concept become very small such that in practice they would not be relevant to safety anymore. We further set the minimum vortex age to 60 s as a value supporting minimum radar separations of 2.5 nm. Operationally WSVS separations below 60 s would not be applicable and adjusted upward to 60 s. In the real-world reference data [44] separation times vary between 80 s and 500 s (see Figure 2 in Ref. [44]). So, within the lidar reference data the flown aircraft separations were consistently larger than those applied in the current Monte Carlo study.

Fig. 2 illustrates the elements employed in the Monte Carlo simulation conducted for the initially available 78,119 aircraft pairings of the Vienna data base. For every predicted WSVS separation, the stochastic leader aircraft position (blue + symbol) and the wake vortex positions are generated for the flight altitude of 50 m above ground targeted by the lidar study. The follower aircraft position (black + symbol) is computed as random deviation from the glide path position using the glide path adherence statistics introduced in the previous section. The stochastic wake vortex positions (* symbols) are generated employing the deterministic vortex positions (o symbols) and the respective standard deviations predicted by the P2P model. Fig. 3 delineates the resulting wake vortex positions with respect to the follower aircraft positions (centered in the origin) at the aircraft separation times suggested by the WSVS.

From this data the distance between the aircraft position and the closest neighboring vortex position, Δr, is determined (see Fig. 2). The distribution of the distances, Δr, is compared to the findings from the lidar airport trials. For the WSVS predictions wake vortices still reside within a distance of 50 m to the follower aircraft in 1.3% of the landings. This is about three times less frequent than the 3.7% estimated by the lidar data analysis. The respective values for a 25 m radius are 0.25% for the Monte Carlo simulation and 1.5% for the real-world reference. Based on this even more safety relevant measure, wake encounters with WSVS separations would be even 6 times less frequent than in daily routine without a wake vortex advisory system.

Long-term lidar measurements of wake vortices at Charles de Gaulle Airport suggest that in 3% of the cases the vortices were at least as close as 25 m in radial distance to the following landing aircraft in proximity of the threshold.[1] Using this finding as a reference to the current simulations must be done with care, because the details of the measurement situation are not known and may deviate from those applied for the Monte Carlo analysis. But it can be considered an additional source suggesting that the chosen settings of the WSVS may deliver reasonably safe pairwise dynamic aircraft separations that are at least as safe as currently used separations.

4. WSVS predictions at windy days

For three selected days of the total period considered, case studies on the actually flown aircraft separations during final approach at Vienna airport and the respective separations predicted by the WSVS are depicted in Fig. 4 to Fig. 6 together with the prevailing meteorological conditions. Panel (a) of the respective figure plots the number of landing aircraft per hour where blue bars denote the fraction of light (L) and medium (M) aircraft and red bars denote the fraction of the heavy (H) and super-heavy (J) aircraft. Panel (b) shows the predicted vertical wind profiles in terms of wind barbs and color-coded headwinds, where winds in flight direction have a positive sign. Wind barbs show both wind direction and speed where each half flag depicts 5 kt and each full flag 10 kt. Panel (c) displays color-coded crosswind profiles and is otherwise equivalent to panel (b). Panel (d) displays the vertical profiles of potential temperature, a parameter controlling wake vortex descent distances and decay rates [7]. Panel (e) denotes hourly distributions of the spatial separations of the landing aircraft pairs derived from Mode-S aircraft position data. The spatial separation between aircraft is determined at the instant when the leader passes the runway threshold. Several significant percentiles of the aircraft separations are denoted as follows: black lines (0^{th} and 100^{th} percentile), light gray bars (5^{th} and 95^{th} percentile), dark gray bars (25^{th} and 75^{th} percentile) and red dashes for the medians. The separations behind leading aircraft of the categories H and J are denoted individually by blue dots. The blue dotted horizontal line indicates the separation between heavy and medium aircraft prescribed by ICAO whereas the minimum radar separation of 2.5 nm is highlighted in gray. Panel (f) corresponds to the same illustration for the WSVS predictions. Here the temporal WSVS separations, t_{sep}, are translated into spatial separations by computing the distance between the positions of the follower aircraft at its touchdown and at t_{sep} before touchdown. Panels (g) and (h) correspond to (e) and (f) for temporal aircraft separations. Highlighted in gray are minimum separations of 1 min corresponding to our approximation of minimum radar separation (see section 3).

Fig. 4 shows a diurnal survey on landing rates, meteorological conditions, and aircraft separations for landings on runway 34 on 18 November 2017. As in the case studies presented in Fig. 5 and Fig. 6, the moderate landing rates throughout most of the day are far below the maximum capacity of the airport of 44 landings per hour. During phases of rather low demand there is no need for controllers to stagger aircraft optimally. Nevertheless, times of higher demand are clearly correlated with smaller aircraft separations, as it is the case on 18 Nov 2017 between 7 and 9 UTC (local morning) (see Fig. 4 e and g).

Fig. 4 demonstrates nicely how the wind conditions impact the WSVS separation reduction potential. Between 6 and 12 UTC sign changes within the crosswind profiles prevent that the vortices are blown out laterally of the flight corridor in some of the WSVS com-

[1] Personal communication with Vincent Treve (EUROCONTROL) during WakeNet3-Europe Workshop, London, 2011.

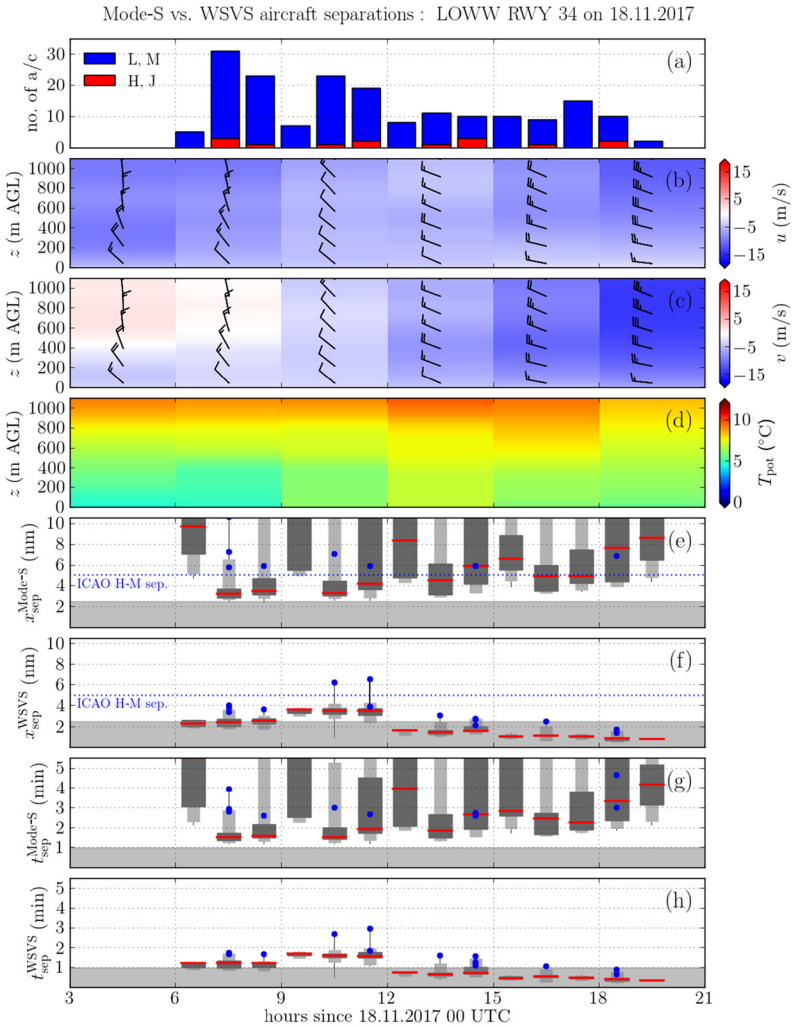

Fig. 4. Case study of landing aircraft, meteorological conditions, and aircraft separations for Vienna Airport runway 34 on 18 November 2017 03-21 UTC. Landing rates (a); wind barbs and headwind profiles (b); wind barbs and crosswind profiles (c); potential temperature profiles (d); 0^{th}, 5^{th}, 25^{th}, 50^{th}, 75^{th}, 95^{th}, and 100^{th} percentiles of the distributions of spatial (e, f) and temporal (g, h) aircraft separations as measured through Mode-S (e, g) and predicted by the WSVS (f, h). Blue bullets in panels (e-h) mark the separations of individual H-M or J-M pairs.

putation gates. Headwinds increase with height from about −3 to −10 m/s such that the respective gates are released earlier by vortex descent. Due to the headwind advection against flight direction the vertical distance between the vortices and the tilted glide path increases with time which can be considered a favorable wake altitude adjustment equivalent (see section 5.1). Eventually, crosswind advection in ground proximity controls the resulting WSVS separations. Between 6 and 9 UTC the slightly stronger surface crosswinds of −1.7 m/s enable somewhat shorter separations compared to the weaker surface crosswinds of only −1.2 m/s prevailing afterwards. The most interesting change in wind conditions occurs starting at 12 UTC (local noon), when the crosswind strength increases all along the vertical profiles. After 18 UTC surface crosswinds are freshening up to −3.6 m/s such that separations are limited by radar separation rather than wake vortex avoidance.

Fig. 5 shows the case study for runway 34 on 30 November 2017. This day comprises the examples of wake vortex predictions discussed in the next section in Fig. 7 to Fig. 12. In the first three-hour time block, 6-9 UTC, the surface crosswinds are close to zero yielding no separation reduction potential compared to ICAO separations. Later on, from 9 to 15 UTC, surface crosswinds on the order of −1.2 m/s slightly improve the separation reduction potential. The single extraordinarily small WSVS separation value of only 5 s is attributed to a Cessna Citation aircraft (ICAO Doc 8643 Aircraft Type Designator: C525) following a Cessna Citation Excel (C56X) between 14 and 15 UTC with a maximum landing weight of only 8.5 t. Only after 15 UTC surface crosswinds of −3.8 m/s and similar strength aloft combined with headwinds stronger than −3 m/s enable separations below 1 min for all aircraft, including heavy leaders.

Fig. 6 depicts the situation for 4 December 2017 where surface headwinds above −3.6 m/s and surface crosswinds above −4.1 m/s combined with substantially higher values aloft for both wind components prevail consistently between 6 and 21 UTC. This constitutes an example where the wind conditions would enable adjusting minimum radar separations for all landing aircraft throughout the day including super heavy leaders followed by medium weight class aircraft.

5. Wind effects on aircraft separations

5.1. Headwind

To better understand the mechanisms controlling temporal aircraft separations in headwind situations we take a closer look at a few selected cases. Fig. 7 to Fig. 9 depict the wake vortex parameters (deterministic predictions of port (magenta) and starboard (blue) vortex and probabilistic one-σ envelope (green)) and safety

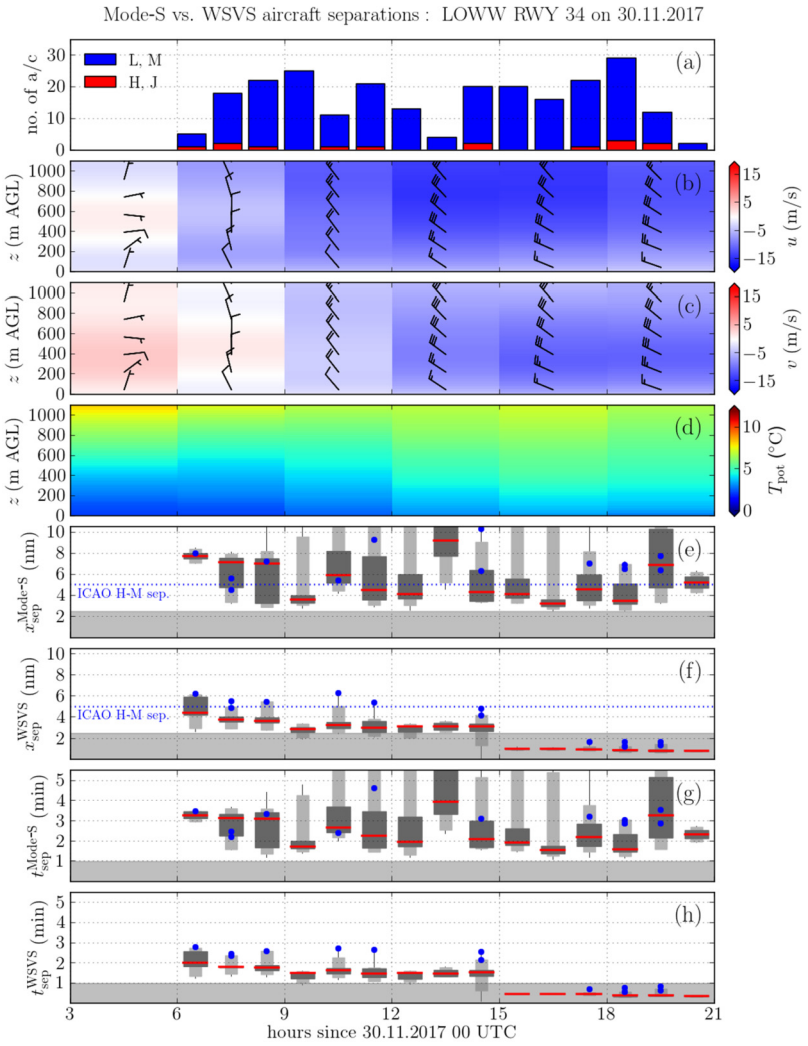

Fig. 5. Same as Fig. 4 but for 30 November 2017 03-21 UTC.

areas (red) for a leading CRJ9 followed by an A320 resulting in the shortest separation of 83.6 s predicted within the time block from 6-9 UTC on 30 November 2017 (cf. Fig. 5). The vertical profiles of the meteorological parameters displayed in the following figures (lower right panels) are normalized employing characteristic wake vortex scales [21]. Here u^* denotes the normalized longitudinal wind component which is positive in flight direction, v^* the cross-wind, q^* the turbulence velocity, N^* the Brunt-Väisäla frequency characterizing thermal stability, and ϵ^* the turbulence energy dissipation rate. Velocities are normalized by the initial wake vortex descent speed, w_0, the Brunt-Väisäla frequency with the initial time, t_0, the vortices need to descend one vortex separation, b_0, and the dissipation rate with $b_0^{1/3}/w_0$.

The instant when all the resulting safety areas (red) along the glideslope have escaped from the approach corridor (dotted lines) either vertically or laterally defines the temporal separation between an individual aircraft pairing. With respect to vortex descent usually the gates aloft without ground effects are first cleared from wake vortices. For example, in gate 7, displayed in Fig. 7, the probabilistic vortex area predicted by the P2P model exits the approach corridor at 24 s and the safety area predicted by the SHAPe model exits the approach corridor at 47 s. So, considering only gate 7, aircraft separations could be adjusted to 47 s.

The prevailing headwind of about four vortex descent speeds ($u \approx -4.7$ m/s) accelerates the unblocking of the approach corridor. Due to the headwind advection against flight direction the vertical distance between vortex area and the 3° glide path increases with time which is reflected by the inclination of the approach corridor plotted in Fig. 7, upper left panel. Laterally the approach corridor is cleared from the safety area only at 137 s due to the weak prevailing crosswind (Fig. 7, upper right panel). The upper one-σ bound (green) of the circulation evolution falls below the deterministic prediction (blue) during the onset of rapid decay owing to the method employed for the training of the probabilistic bounds with measurement data. The lower circulation envelopes are not shown, because they are not used for the WSVS predictions.

Fig. 8 displays WSVS predictions in ground proximity in gate 14. Due to the interaction with the ground, vortex descent is limited. Instead the vortices diverge and rebound [8], [9] such that the upper probabilistic bound resides eventually slightly below 30 m. Due to the headwind transport the shrinking safety area exits the approach corridor at about 77 s. Due to weak crosswinds and vortex divergence in ground proximity even the probabilistic vortex envelopes don't leave the approach corridor laterally.

Fig. 9 illustrates that in the lowest gate 15 the safety area cannot exit the approach corridor vertically within a relevant period of time despite the headwind effect due to vortex rebound and the low flight altitude. Here the aircraft separation is controlled by vortex decay. At 84 s the vortices have decayed sufficiently that the roll control ratio has dropped below 0.2 and the following A320 aircraft may land without compromising safety. So, with

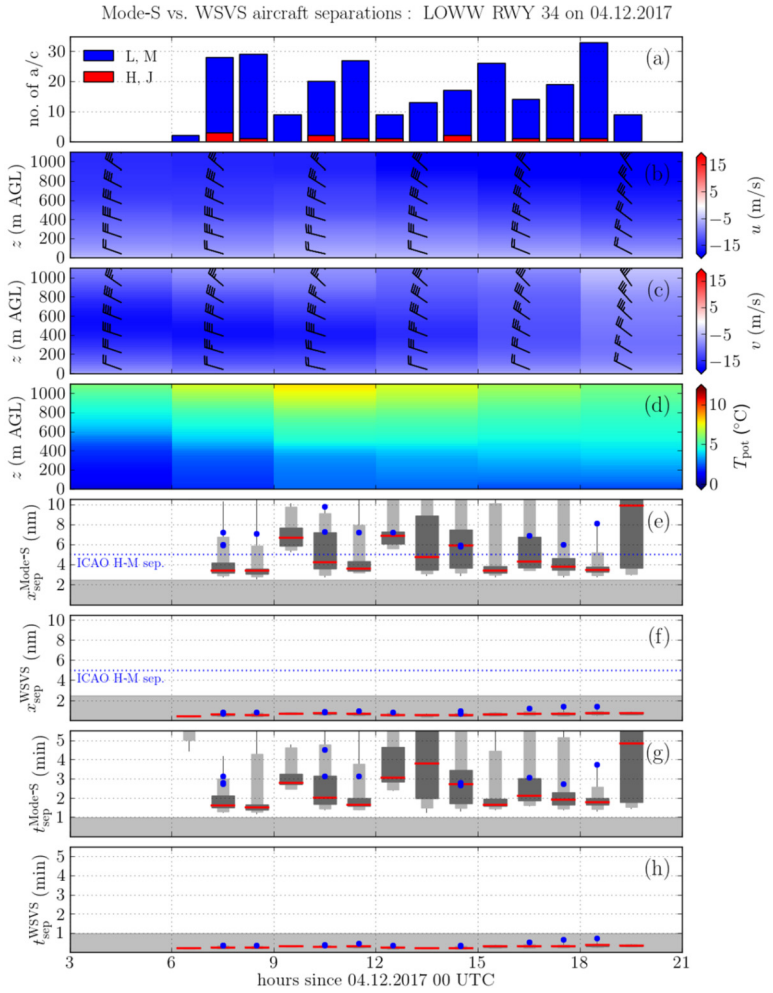

Fig. 6. Same as Fig. 4 but for 4 December 2017 03-21 UTC.

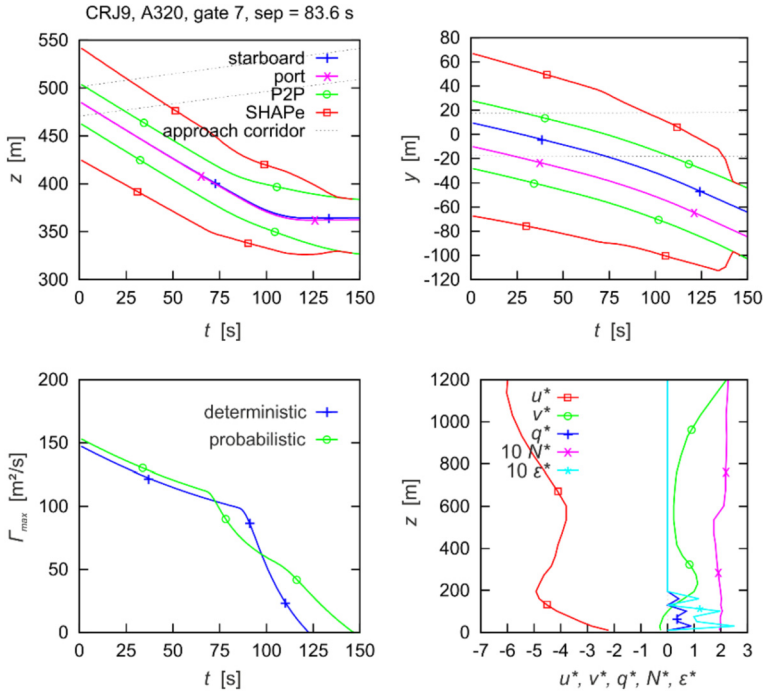

Fig. 7. WSVS prediction of wake vortex parameters, safety areas and meteorological parameters for a leading CRJ9 followed by an A320 in gate 7. Approach corridor cleared from safety area at 47 s by descent (top left).

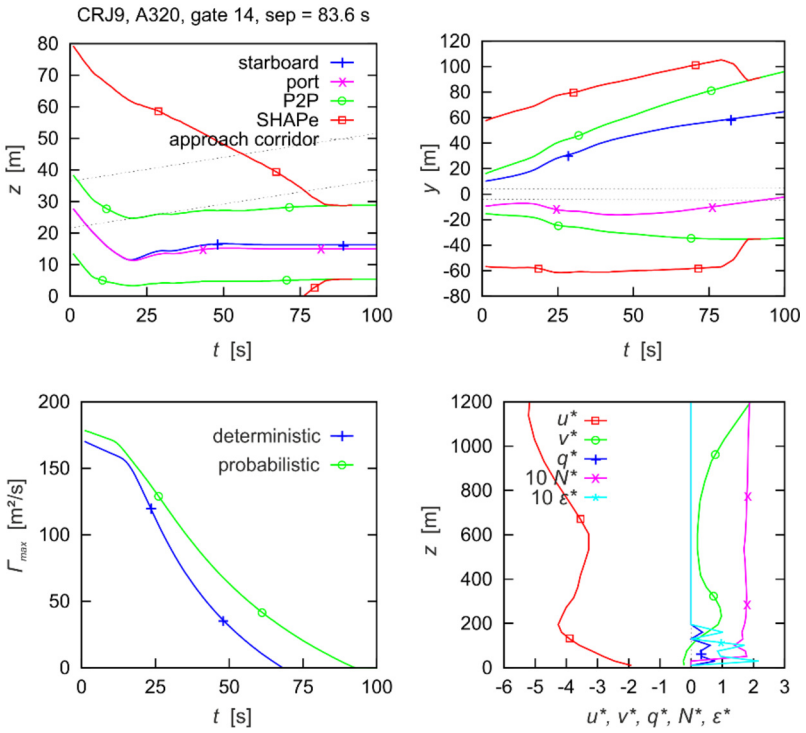

Fig. 8. WSVS prediction of wake vortex parameters, safety areas and meteorological parameters for a leading CRJ9 followed by an A320 in gate 14. Approach corridor cleared from safety area at about 77 s (top left).

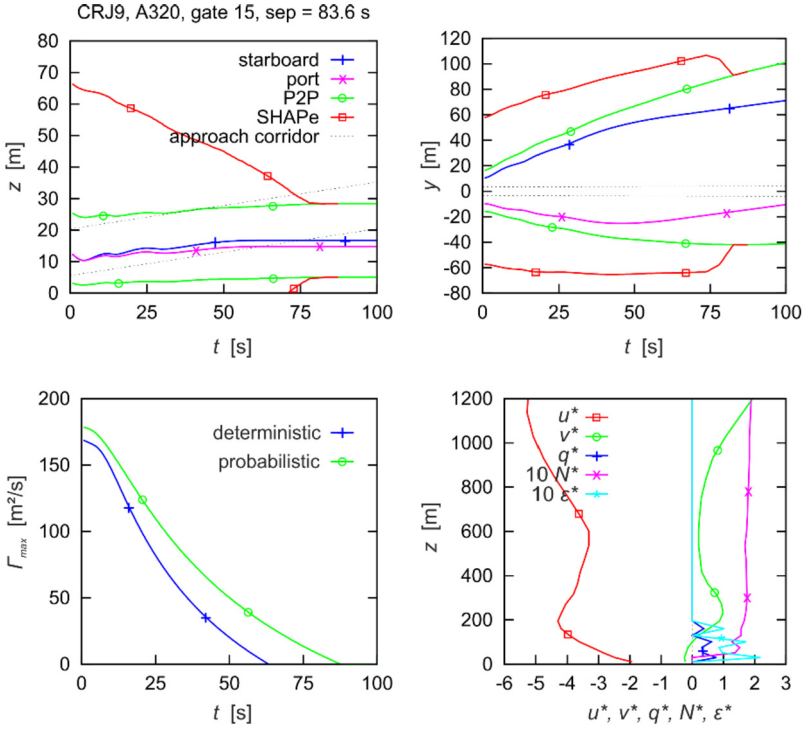

Fig. 9. WSVS prediction of wake vortex parameters, safety areas and meteorological parameters for a leading CRJ9 followed by an A320 in gate 15. At 84 s the vortices have decayed to a safe level such that the safety area falls on top of the vortex area (top panels).

weak crosswind and intermediate headwind strengths aircraft separations are typically controlled by vortex decay in close ground proximity.

There are also a few cases where the headwind transport is not sufficient to transport the vortices out of the approach corridor even in gate 14. In that situation vortex decay in gate 14 determines the aircraft separations because the vortices generated at very low altitudes above ground (in gate 15) decay faster.

Fig. 10 demonstrates that vortex decay in close ground proximity may vary considerably even for different medium sized aircraft. For the aircraft pairing DH8D/DH8D the vortices have decayed sufficiently only at 168 s. Vortex decay scales with the characteristic

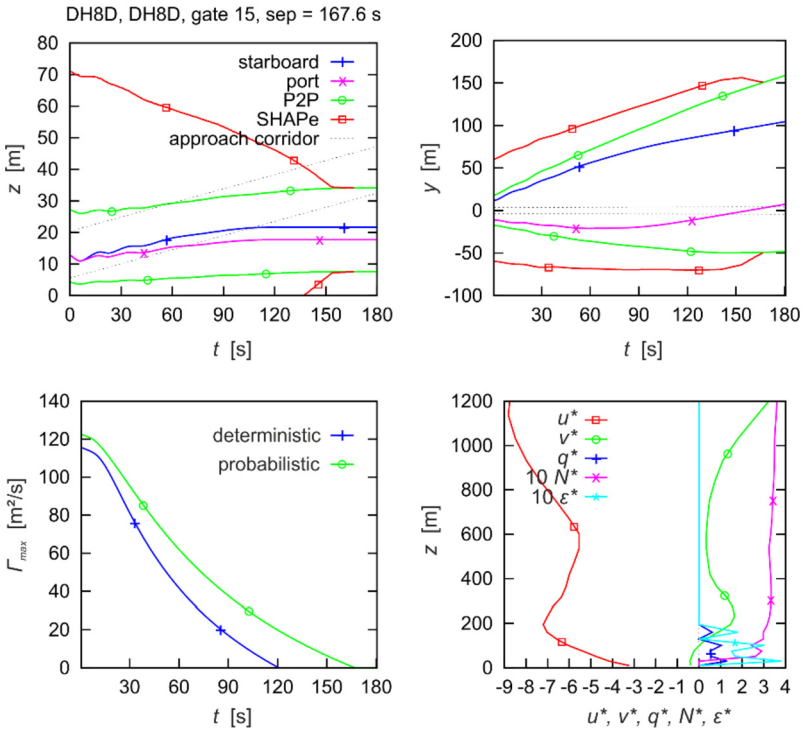

Fig. 10. WSVS prediction of wake vortex parameters, safety areas and meteorological parameters for a leading DH8D followed by another DH8D in gate 15. At 168 s the vortices have decayed to a safe level such that the safety area falls on top of the vortex area (top panels).

vortex time t_0 which amounts to 14 s for the CRJ9 and to 27 s for the DH8D. The relatively high (low) characteristic vortex time of the DH8D (CRJ9) results from its relatively large (small) span of 28.4 m (24.8 m) in relation to its low (high) weight of 28 t (34 t).

During conditions in which aircraft separations are controlled by vortex decay in ground proximity, aircraft separations could be reduced by the installation of plate lines underneath the approach glide path. Lidar measurements conducted at runway 16 of Vienna International Airport indicate that this way the lifetime of the long-lived vortices can be reduced by 21% to 35% depending on the aircraft size. This corresponds to a reduction of vortex circulation by about 50% assuming a 120 s separation between leading heavy and following medium weight class aircraft [47].

5.2. Crosswind

After 15 UTC on 30 November 2017 the wind direction has turned such that the vortex separations are controlled by lateral transport of the wake vortices out of the flight corridor (see Fig. 5). The crosswind profile exhibits a maximum absolute value ($u = -11.4$ m/s) at an altitude of 367 m and minimum absolute values (-4.4 m/s) both at the ground and at the beginning of the considered glide path. Depending on the aircraft size either gate 1 or gate 15 (both close to the crosswind minima) control reduced aircraft separations.

Fig. 11 shows an example for a leading medium aircraft. Here the safety area leaves the flight corridor, which is the widest in gate 1, laterally at a vortex age of 23 s. In all other gates the flight corridor is cleared earlier due to its smaller width and the mostly larger crosswind. Fig. 12 displays an example with a leading B744 where the safety area ultimately quits the lowest gate 15 at 39 s. For big aircraft in this meteorological situation the larger initial vortex separation and vortex divergence in ground proximity are decisive. In such cases the aircraft separations could be reduced from 5 nm (ICAO separation) to a minimum radar separation of 2.5 nm for leading heavy aircraft followed by mediums.

5.3. Veering winds

The direction of the wind varies with the height above ground. According to the concept of the Ekman spiral the wind direction turns to the right with increasing height as it is the case in Fig. 11 to Fig. 14. Above the atmospheric boundary layer with a thickness on the order of 1 km, the wind direction is mainly controlled by the equilibrium of the driving pressure gradient force and the Coriolis force. The resulting wind is called geostrophic wind. In the atmospheric boundary layer, the friction force causes a deviation of the wind direction to the left (on the northern hemisphere).

Specifically, at Vienna airport abrupt vertical wind direction changes are frequently related to vertical air mass boundaries. Typically, southeasterly winds at lower altitudes are eroded by westerly winds from above. This may lead to situations where favorable headwind conditions in ground proximity are combined with adverse tailwinds aloft.

Fig. 13 illustrates a pronounced headwind situation with up to 11 m/s and a crosswind component below 400 m altitude with a maximum of 3.8 m/s prevailing on 18 November 2017 during the time block starting at 21 UTC. The headwind in ground proximity of about 4 m/s is not strong enough to transport the rebounding A319 wake vortices sufficiently far against flight direction such that the flight corridor would be cleared from the vortices. However, the crosswind of 2.6 m/s advects the safety area out of the flight corridor at 62 s. The flight corridor in gate 1 is freed from the safety corridor only at 79 s where the headwind strengthens the effective vortex descent of the barely attenuated vortices (see Fig. 14).

6. Statistics of wind effects on aircraft separations

As described in the previous sections, the minimum wake turbulence separations predicted by the WSVS dominantly depend on the wind conditions as well as the wake vortex characteristics. The latter in turn depend on the aircraft type and its operating

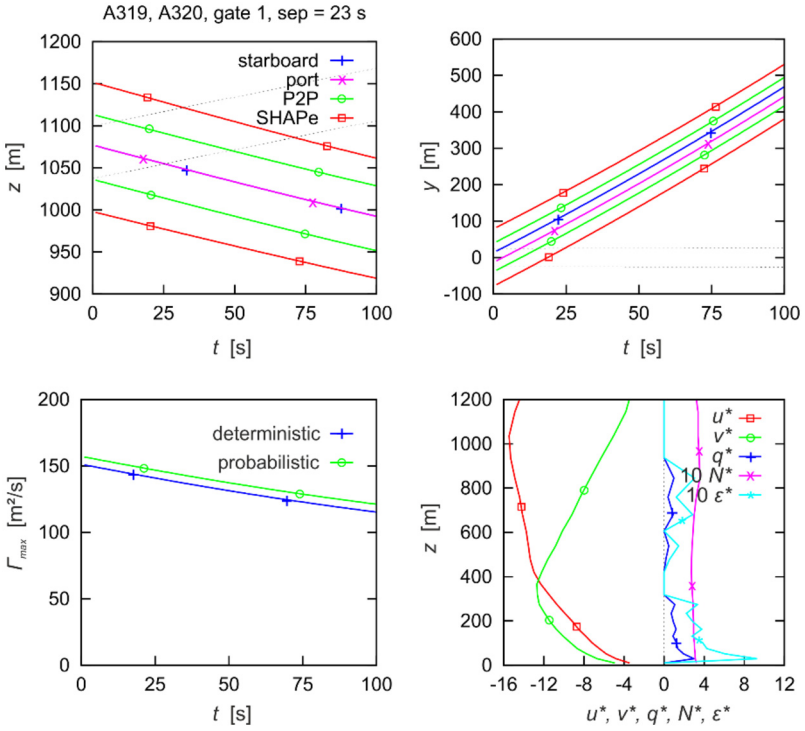

Fig. 11. WSVS prediction of wake vortex parameters, safety areas and meteorological parameters for a leading A319 followed by an A320 in gate 1. Safety area leaves flight corridor laterally at vortex age of 23 s (top right).

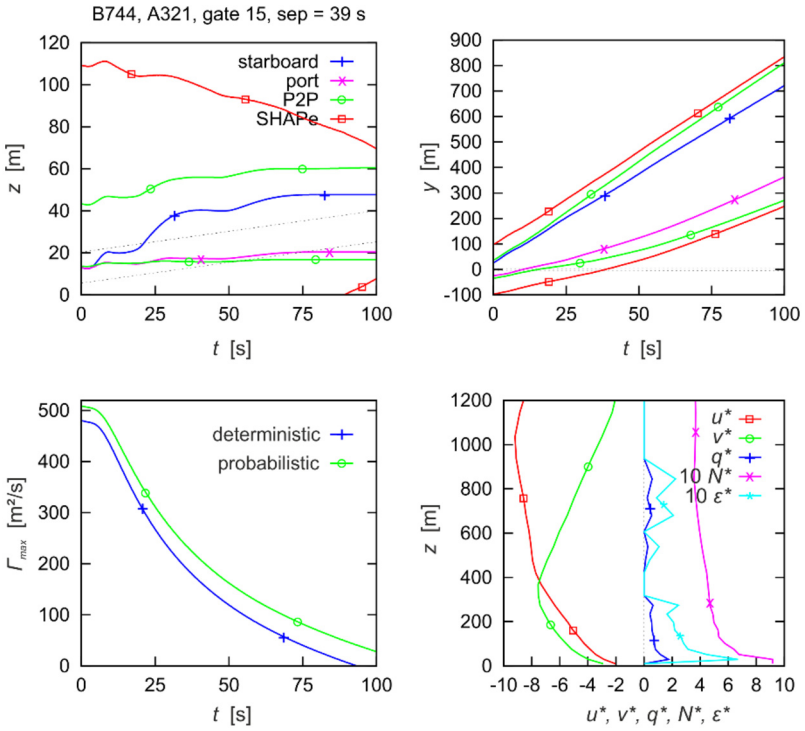

Fig. 12. WSVS prediction of wake vortex parameters, safety areas and meteorological parameters for a leading B744 followed by an A321 in gate 15. Safety area leaves flight corridor laterally at vortex age of 39 s (top right).

conditions and also the follower aircraft type which impacts the size of the safety area. Fig. 15 shows mean values of the WSVS separation times of 106,293 aircraft pairings as a function of headwind and crosswind speeds. Wind speeds are taken from the reference height of the last unblocked gate (see Table 1). Because the data base mainly contains medium weight class aircraft, these mean separations correspond exclusively to landings with medium weight class leader and follower aircraft. Headwinds are denoted by negative values of u. Wind conditions not covered by landings are denoted by separation times of 0 s.

Obviously, crosswinds are most efficient in advecting the vortices away from the flight corridor. On average, crosswinds above

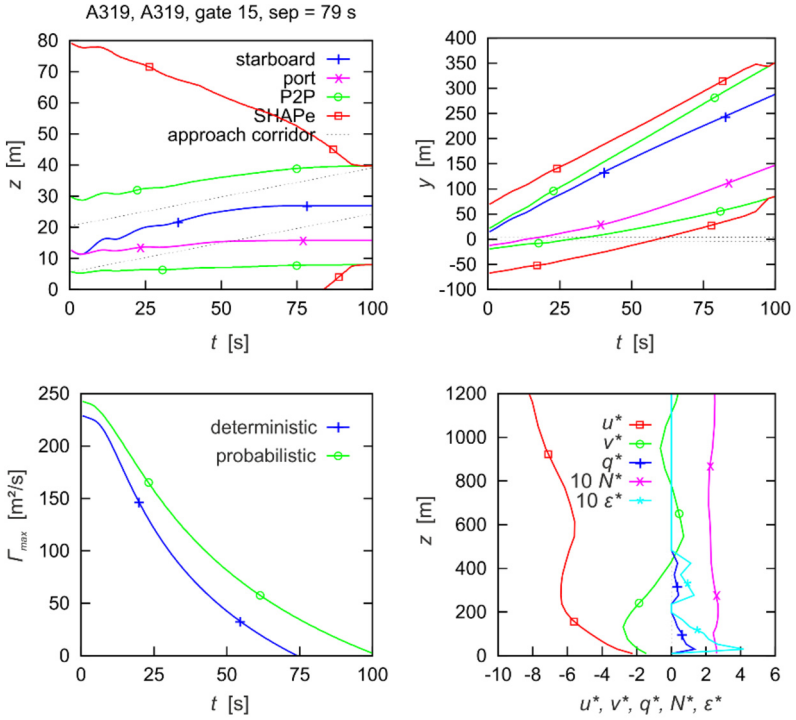

Fig. 13. WSVS prediction of wake vortex parameters, safety areas and meteorological parameters for a leading A319 followed by an A319 in gate 15. Crosswind advects safety area out of flight corridor at 62 s (top right).

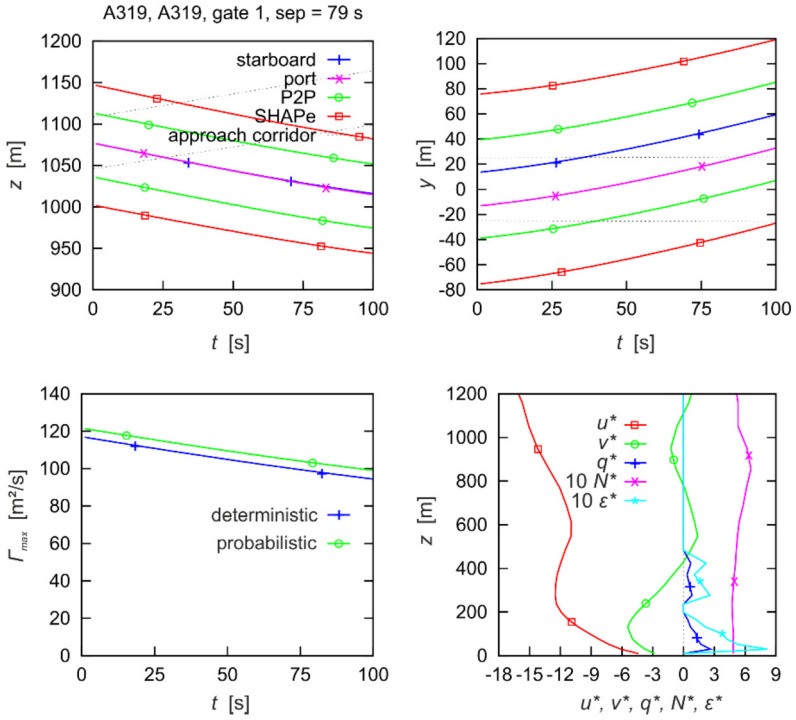

Fig. 14. WSVS prediction of wake vortex parameters, safety areas and meteorological parameters for a leading A319 followed by an A319 in gate 1. Approach corridor cleared from safety area at 79 s by descent supported by the headwind (top left).

±2 m/s are sufficient to reduce separation times to about 1 min. At typical aircraft speeds during final approach of 160 kt and zero headwind component, a time separation of 1 min corresponds to approximately 2.5 nm, the minimum radar separation applicable when wake vortex separation is not required. As explained in section 4, headwinds accelerate the unblocking of the approach corridor by advecting the vortices along the direction of the sloping glide path. So, headwind advection can be considered to act as an increased vortex descent speed. Tailwinds have the opposite effect for what reason maximum average separations of 170 s occur around tailwinds of 8 m/s with crosswinds close to zero. The effect of headwinds on acceptable aircraft separations, however, is indirect and thus small. Only for headwinds stronger than −15 m/s the average separation times drop below 1 min.

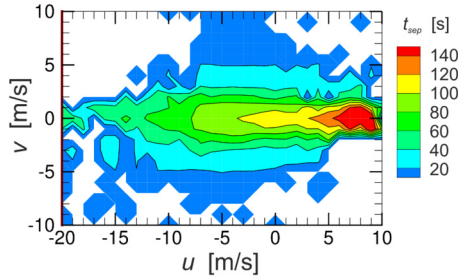

Fig. 15. WSVS mean separations as a function of wind speeds in last cleared gates.

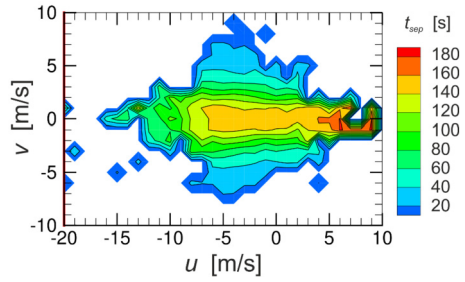

Fig. 16. WSVS mean separations as a function of wind speeds in last cleared gates for medium aircraft behind heavies.

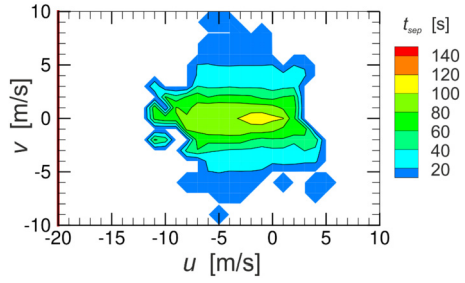

Fig. 17. WSVS mean separations as a function of wind speeds in the last gate before touchdown.

The count of medium aircraft behind heavy aircraft amounts to only 5901 or 5.5% of the considered landings. As a consequence, the corresponding mean separation times plot shown in Fig. 16 is less smooth and covers smaller ranges of wind speeds. For heavy-medium pairings crosswinds of at least ±4 m/s are needed to consistently reduce mean separation times to about 1 min. The data base is not big enough to derive a reliable headwind threshold above which aircraft separations fall below one min. At tailwinds of 6 m/s combined with neglectable crosswinds mean time separations arrive at the adjusted maximum prediction time of the WSVS of 180 s.

In 69% of the cases, the wake behavior in gate 15 closest to the ground controls minimum wake turbulence separations because in close ground proximity vortices cannot descend below the flight corridor and lateral vortex advection of the luff vortex is partly compensated by vortex induced lateral propagation [8], [9] (cf. e.g. Fig. 9). Fig. 17 illustrates the wind conditions when gate 15 is cleared last by the safety areas. Due to the ground proximity the data base does not contain situations with winds above 11 m/s and tailwinds are largely limited to 4 m/s. Maximum mean separation times of around 110 s occur for weak headwinds and zero crosswinds. Due to the interaction with the ground the mean crosswind needed to enable aircraft separations below 1 min amounts to 3 m/s, which is 1 m/s more than in Fig. 15.

Fig. 18 depicts the 0^{th}, 5^{th}, 25^{th}, 50^{th}, 75^{th}, 95^{th} and 100^{th} percentiles of the predicted WSVS separations as a function of the crosswind speeds in the last cleared gates for the considered land-

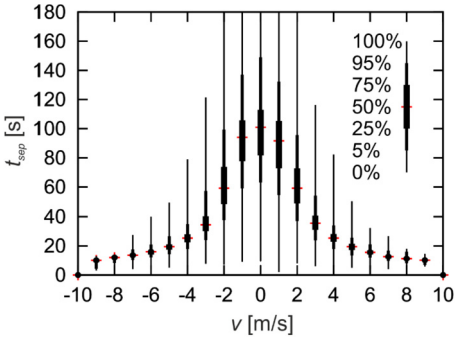

Fig. 18. Percentiles of predicted WSVS separations as a function of crosswind speeds in last cleared gates.

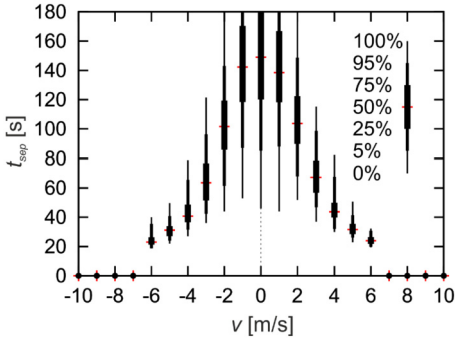

Fig. 19. Percentiles of predicted WSVS separations as a function of crosswind speeds in last cleared gates for medium aircraft behind heavies.

ings. In the zero-crosswind class, the whole range of separation times between 10 s and 180 s is present depending on aircraft type combinations and meteorological conditions, where headwind effects contribute dominantly to that large spread. The median value denoted by the red dash amounts to 101 s. As seen already in Fig. 15, the median separation times drop below 60 s at crosswinds of about ±2 m/s, a crosswind speed where the maximum separation times are still cut off at 180 s, due to the adjusted maximum prediction time of the WSVS. Crosswinds of at least ±3 m/s (±5 m/s) are necessary to separate 95% (all) of the landing aircraft by less than 1 min. Crosswinds of ±9 m/s blow the safety areas out of the flight corridor in less than 15 s.

Fig. 19 shows the same dependencies as Fig. 18 for medium aircraft behind heavies. Since the calculation of the 5^{th} and the 95^{th} percentiles require at least 20 cases, the maximum crosswinds are limited to ±6 m/s. The maximum separation values in Fig. 18 and Fig. 19 are identical because they are controlled by medium aircraft following heavies or super-heavies. However, all other separation values are substantially increased because of the higher values of initial circulation and vortex separation of the trailing vortices generated by the larger aircraft. Nevertheless, the result from Fig. 18 that crosswinds of at least ±5 m/s are required to separate all of the landing aircraft by less than 1 min holds also for this class of pairings.

Fig. 20 delineates headwind effects on WSVS separations. For a wide range of headwind speeds the separation times vary between very small values and the adjusted maximum of 180 s. So, a headwind threshold alone is generally not suitable to reduce aircraft separations. Nevertheless, the median separation times decrease almost linearly with increasing headwind speeds. In combination with other favorable parameters like crosswind, headwinds may contribute to some helpful reduction of separations (cf. headwind range below −7 m/s in Fig. 15).

Fig. 21 shows statistics of the predicted WSVS separations dependent on the minimum crosswind magnitude within the entire

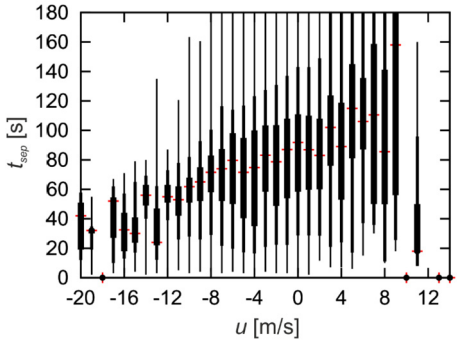

Fig. 20. Predicted WSVS separations as a function of headwind speeds in last cleared gates; 0^{th}, 5^{th}, 25^{th}, 50^{th}, 75^{th}, 95^{th} and 100^{th} percentiles.

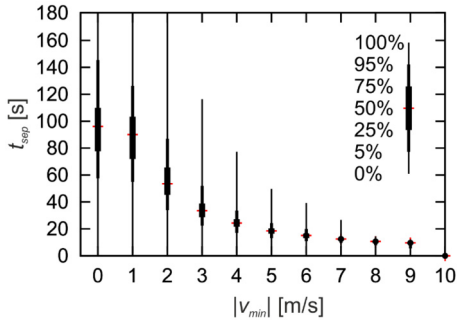

Fig. 21. Percentiles of predicted WSVS separations as a function of minimum crosswind magnitude along the entire height range covered by the gates.

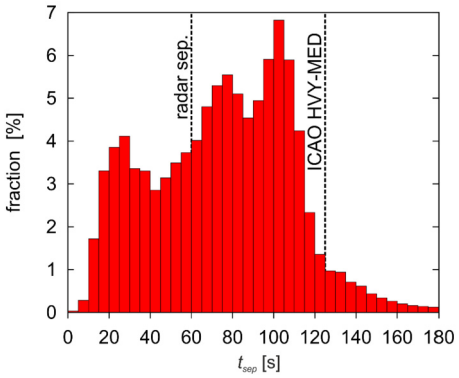

Fig. 22. Distribution of temporal aircraft separations suggested by the WSVS.

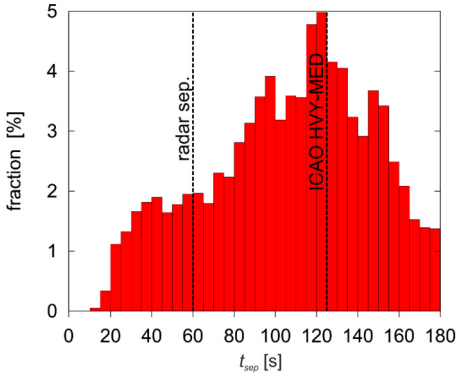

Fig. 23. Distribution of temporal aircraft separations suggested by the WSVS for heavy/medium aircraft sequences.

wind profile within the height range covered by the gates. On average, the minimum crosswind within the whole vertical crosswind profile needed to allow for a certain aircraft separation is only slightly lower than the crosswind in the gate that is cleared last. This means that for most cases the last cleared gate corresponds to the gate residing closest to the crosswind minimum within the considered height range. Accordingly, the percentiles for the aircraft separations at a given crosswind minimum are slightly lower than those interpolated to the relevant gate (cf. Fig. 18).

From Fig. 21 it can be concluded that crosswind magnitudes of at least 5 m/s all along a vertical crosswind profile are sufficient to separate all landing aircraft by less than 1 min without the need to operate a wake vortex advisory system. However, this favorable situation, where aircraft separations could be reduced significantly based on a simple crosswind criterion, prevails only during 4.7% of the investigated cases. As detailed in the following section, the operation of the WSVS could increase this percentage substantially to 33% of the landings. Crosswinds of at least 3 m/s occurring during 19.6% of the cases enable to separate 95% of the landing aircraft by less than 1 min.

An analysis for departures at Frankfurt airport yields a crosswind threshold of 8 kt (4.1 m/s) measured at an altitude of 10 m above ground to reduce the associated separation distances between heavy leader aircraft and medium follower aircraft from the required 2 min to only 1 min [48], [49]. The departure study stipulated that for 1 min separations under favorable crosswind conditions the encounter risks (derived from encounter frequency and severity) were lower than those in a reference scenario at 2 min separations.

7. Separation-reduction potential

Fig. 22 displays the distribution of temporal separations suggested by the WSVS for all 106,293 aircraft pairings. The fraction of landings below minimum radar separation (corresponding to approximately 60 s) amounts to 33%. Fig. 23 displays the predicted aircraft separations for heavy vortex generators and medium follower aircraft. In 55% of landings separations could be reduced below a value of 125 s being representative for the 5 nm separation prescribed by ICAO according to Ref. [28]. It is interesting to note that the peak of the separation distribution in Fig. 23 is situated close to the corresponding value of the ICAO weight class matrix. This may be considered as indication that the heavy/medium ICAO separation was indeed well chosen. The fraction of landings where minimum radar separation of 60 s could be applied amounts to 14%.

The criterion that crosswinds of 5 m/s or stronger prevail along the whole altitude range covered by the WSVS also allows to reduce separations to 60 s without installation of any wake vortex advisory system (see Fig. 21). However, in the Vienna database such favorable winds are present only during 4.7% of the time.

Table 2 lists the spatial separations foreseen by the RECAT-EU scheme [25]. The number of the aircraft pairings where the RECAT-EU scheme could be applied is listed in brackets and sums up to 8.7% of the considered landings. The table further specifies the fraction of time when WSVS predictions would allow reducing the RECAT-EU separations to minimum radar separation of 60 s. On average this is possible in 19% of the cases. The fraction of the total considered traffic where RECAT-EU separations could be reduced to minimum radar separation amounts to 1.6%.

The fraction of time where RECAT-EU can be applied and the corresponding capacity gains vary significantly for different airports depending on their respective traffic mixes [25]. Correspondingly, also the fraction of the air traffic where the WSVS may optimize aircraft separations will highly depend on the considered airport with its specific traffic mix and wind climatology.

The Vienna database does not contain landings with leading category A and following category A. For A leaders followed by cat-

Table 2
RECAT-EU distance-based separation minima and respective fraction of minimum radar separations suggested by the WSVS for the Vienna dataset. Number of landings applying RECAT-EU separations in brackets.

Follower Leader	Super heavy A	Upper heavy B	Lower heavy C	Upper med. D	Lower med. E	Light F
Super heavy A	3 nm –	4 nm 4% (27)	5 nm 0% (1)	5 nm 5% (210)	6 nm 8% (77)	8 nm 0% (12)
Upper heavy B	– –	3 nm 16% (464)	4 nm 11% (267)	4 nm 14% (2393)	5 nm 10% (1448)	7 nm 21% (119)
Lower heavy C	– –	– –	3 nm 14% (205)	3 nm 20% (1118)	4 nm 16% (844)	6 nm 21% (28)
Upper medium D	– –	– –	– –	– –	– –	5 nm 33% (1331)
Lower medium E	– –	– –	– –	– –	– –	4 nm 39% (617)
Light F	– –	– –	– –	– –	– –	3 nm 58% (60)

egory C or F none of the separations of the few recorded landings could be reduced below 60 s. For the other category combinations, the fraction of times supporting minimum radar separation vary between 4% and 58%. For a given follower category, the fraction of reduced separations decreases with increasing weight and span of the leading aircraft types.

8. Conclusion

This study assesses various aspects of the deployment of dynamic pairwise wake vortex separations for approach and landing at Vienna airport using the Wake Vortex Prediction System WSVS.

A Monte Carlo simulation study demonstrates that the WSVS is well adjusted to a reasonable level of safety. The simulation study evaluates the probability that wake vortices linger within a defined radius around the follower aircraft when dynamic pairwise wake vortex separations are applied. This probability is compared to current practice using measurement data collected at five major international airports. It is found that for WSVS predictions wake vortices in ground proximity still reside within a distance of 25 m to the follower aircraft in 0.25% of the landings. This is about six times less frequent than the 1.5% estimated by the independent lidar data analysis representing the daily routine without a wake vortex advisory system. It is concluded that the WSVS may deliver reasonably safe pairwise dynamic aircraft separations that are at least as safe as currently used separations.

The WSVS has been applied to twelve months of traffic and weather prediction data collected at Vienna International Airport. Selected case studies provide overviews on landing rates, meteorological conditions, spatial and temporal aircraft separations as actually flown. These separations are compared to dynamic pairwise wake vortex separations predicted by the WSVS. Favorable wind conditions allow reducing aircraft separations to minimum radar separation for periods of several hours or even complete days.

Individual analyses of different traffic situations and wind conditions reveal which mechanisms and combinations of mechanisms inhibit or facilitate reduced wake turbulence separations. The effects of headwind and crosswind as well as the aircraft type combination on the unblocking of the different prediction planes (gates) along the approach corridor are discussed in detail on the basis of selected individual probabilistic wake vortex predictions and related safety areas. The effect of headwinds on acceptable aircraft separations is fairly small. Intermediate headwinds accelerate the unblocking of the inclined approach corridor but close to the ground vortex descent is inhibited such that, in the absence of sufficiently strong crosswinds, aircraft separation is largely controlled by vortex decay. Only for headwinds stronger than 15 m/s, the average separation time drops below 1 min.

Strong crosswind constitutes the most efficient mechanism to unblock the approach corridor. Here typically either the highest gate controls the aircraft separation, because there the approach corridor is the widest, or the lowest gate is unblocked at last, because of the lower wind speeds in ground proximity and the vortex divergence driven by the interaction with the ground surface. Crosswinds above ± 2 m/s are sufficient to reduce median separation times to about 1 min. However, crosswinds of at least ± 3 m/s (± 5 m/s) are necessary to separate 95% (all) of the landing aircraft by less than 1 min. Crosswinds of ± 9 m/s blow the safety areas out of the flight corridor in less than 15 s. A 5 m/s crosswind threshold blowing all along the glide path supports separations by less than 1 min without the need to operate a wake vortex advisory system. However, such favorable wind conditions prevail only during 4.7% of the investigated cases. The operation of the WSVS could increase this percentage substantially to 33% of the landings.

For 55% of the medium aircraft following heavy vortex generators, the WSVS could reduce landing separations below a value of 125 s (corresponding to the prescribed ICAO separation of 5 nm) and the fraction of landings where minimum radar separation (approximated by 60 s) could be applied amounts to 14%. In 19% of landings, for which RECAT-EU vortex separations apply, a further reduction to minimum radar separation is found to be possible while ensuring safety.

Based on this study's findings, we conclude that the installation of the WSVS for operational purposes may substantially increase the number of aircraft landing on a runway per hour under suitable weather conditions without compromising safety. Further capacity gains could be made accessible by the installation of plate lines [47] underneath the approach glide path which may accelerate wake vortex decay in the lowest three gates controlling minimum wake turbulence separations in 85% of the time.

Declaration of competing interest

The authors declare that they have no known competing financial interests or personal relationships that could have appeared to influence the work reported in this paper.

Acknowledgements

The work was funded by the Federal Ministry of the Republic of Austria for Transport, Innovation and Technology project "MET Potentiale im Arrival- und Departure Management - MET4LOWW"

and the German Aerospace Research Center (DLR) project "Wetteroptimierter Luftverkehr".

References

[1] J.N. Hallock, F. Holzäpfel, A review of recent wake vortex research for increasing airport capacity, Prog. Aerosp. Sci. 98 (2018) 27–36, https://doi.org/10.1016/j.paerosci.2018.03.003.

[2] European Aviation in 2040 - Challenges of Growth, EUROCONTROL, 2018, p. 40, https://www.eurocontrol.int/publication/challenges-growth-2018. (Accessed 15 December 2020).

[3] Y. Wang, M. Abdel-Maksoud, Application of remeshed vortex method for the simulation of tip vortex at high Reynolds number, Aerosp. Sci. Technol. 93 (2019) 105347, https://doi.org/10.1016/j.ast.2019.105347.

[4] C. Breitsamter, Wake vortex characteristics of transport aircraft, Prog. Aerosp. Sci. 47 (2011) 89–134, https://doi.org/10.1016/j.paerosci.2010.09.002.

[5] T. Misaka, S. Obayashi, Numerical study on jet-wake vortex interaction of aircraft configuration, Aerosp. Sci. Technol. 70 (2017) 615–625, https://doi.org/10.1016/j.ast.2017.08.038.

[6] F. Holzäpfel, T. Hofbauer, D. Darracq, H. Moet, F. Garnier, C. Ferreira Gago, Analysis of wake vortex decay mechanisms in the atmosphere, Aerosp. Sci. Technol. 7 (2003) 263–275, https://doi.org/10.1016/S1270-9638(03)00026-9.

[7] F. Holzäpfel, Effects of environmental and aircraft parameters on wake vortex behavior, J. Aircr. 51 (2014) 1490–1500, https://doi.org/10.2514/1.C032366.

[8] F. Holzäpfel, M. Steen, Aircraft wake-vortex evolution in ground proximity: analysis and parameterization, AIAA J. 45 (2007) 218–227, https://doi.org/10.2514/1.23917.

[9] F. Holzäpfel, N. Tchipev, A. Stephan, Wind impact on single vortices and counterrotating vortex pairs in ground proximity, Flow Turbul. Combust. 97 (2016) 829–848, https://doi.org/10.1007/s10494-016-9729-2.

[10] W. He, P. Yu, L.K.B. Li, Ground effects on the stability of separated flow around a NACA 4415 airfoil at low Reynolds numbers, Aerosp. Sci. Technol. 72 (2018) 63–76, https://doi.org/10.1016/j.ast.2017.10.039.

[11] Q. Chen, T. Hu, P. Liu, Y. Liu, Q. Qu, H. Guo, R.A.D. Akkermans, Experiments on asymmetric vortex pair interaction with the ground, Exp. Fluids 61 (2020) 150, https://doi.org/10.1007/s00348-020-02987-7.

[12] Y. Wang, P. Liu, T. Hu, Q. Qu, Q. Chen, R. Akkermans, Experimental investigations on the interaction of the single/co-rotating vortex with the ground, AIAA J. 57 (2019) 499–512, https://doi.org/10.2514/1.J057140.

[13] A. Stephan, F. Holzäpfel, T. Misaka, Hybrid simulation of wake-vortex evolution during landing on flat terrain and with plate line, Int. J. Heat Fluid Flow 49 (2014) 18–27, https://doi.org/10.1016/j.ijheatfluidflow.2014.05.004.

[14] F. Holzäpfel, A. Stephan, T. Heel, S. Körner, Enhanced wake vortex decay in ground proximity triggered by plate lines, Aircr. Eng. Aerosp. Technol. 88 (2) (2016) 206–214, https://doi.org/10.1108/AEAT-02-2015-0045.

[15] F. Holzäpfel, M. Frech, T. Gerz, A. Tafferner, K.-U. Hahn, C. Schwarz, H.-D. Joos, B. Korn, H. Lenz, R. Luckner, G. Höhne, Aircraft wake vortex scenarios simulation package – WakeScene, Aerosp. Sci. Technol. 13 (2009) 1–11, https://doi.org/10.1016/j.ast.2007.09.008.

[16] X. Olive, J. Morio, Trajectory clustering of air traffic flows around airports, Aerosp. Sci. Technol. 84 (2019) 776–781, https://doi.org/10.1016/j.ast.2018.11.031.

[17] J. Cho, B.J. Lee, T. Misaka, K. Yee, Study on decay characteristics of vertical four-vortex system for increasing airport capacity, Aerosp. Sci. Technol. 105 (2020) 106017, https://doi.org/10.1016/j.ast.2020.106017.

[18] G.C. Greene, An approximate model of vortex decay in the atmosphere, J. Aircr. 23 (1986) 566–573.

[19] L.H. Kantha, Empirical model of transport and decay of wake vortices between parallel runways, J. Aircr. 33 (1996) 752–760, https://doi.org/10.2514/3.47011.

[20] F.H. Proctor, The NASA-Langley Wake Vortex Modelling Effort in Support of an Operational Aircraft Spacing System, AIAA Paper 1998-0589, January 1998.

[21] F. Holzäpfel, Probabilistic two-phase wake vortex decay and transport model, J. Aircr. 40 (2003) 323–331, https://doi.org/10.2514/2.3096.

[22] F.H. Proctor, D.W. Hamilton, G.F. Switzer, TASS Driven Algorithms for Wake Prediction, AIAA Paper 2006-1073, January 2006.

[23] I.G. De Visscher, G. Winckelmans, T. Lonfils, L. Bricteux, M. Duponcheel, N. Bourgeois, The WAKE-4D Simulation Platform for Predicting Aircraft Wake Vortex Transport and Decay: Description and Examples of Application, AIAA Paper 2010-7994, August 2010.

[24] J. Cheng, J. Tittsworth, W. Gallo, A. Awwad, The Development of Wake Turbulence Recategorization in the United States, AIAA Paper 2016-3434, June 2016, p. 12.

[25] RECAT-EU, European Wake Turbulence Categorisation and Separation Minima on Approach and Departure, EUROCONTROL, 2015, p. 32, https://www.eurocontrol.int/publication/european-wake-turbulence-categorisation-and-separation-minima-approach-and-departure. (Accessed 29 June 2020).

[26] Aircraft Wake Vortex State-of-the-Art & Research Needs, WakeNet3-Europe, compiled by F. Holzäpfel, et al., issued by A. Reinke, C. Schwarz, November 2015, p. 201, https://doi.org/10.17874/BFAEB7154B0. (Accessed 29 June 2020).

[27] F. Holzäpfel, T. Gerz, M. Frech, A. Tafferner, F. Köpp, I. Smalikho, S. Rahm, K.-U. Hahn, C. Schwarz, The wake vortex prediction and monitoring system WSVBS - Part I: design, Air Traffic Control Q. 17 (4) (2009) 301–322, https://doi.org/10.2514/atcq.17.4.301.

[28] T. Gerz, F. Holzäpfel, W. Gerling, A. Scharnweber, M. Frech, K. Kober, K. Dengler, S. Rahm, The wake vortex prediction and monitoring system WSVBS Part II: performance and ATC integration at Frankfurt airport, Air Traffic Control Q. 17 (4) (2009) 323–346, https://doi.org/10.2514/atcq.17.4.323.

[29] F. Holzäpfel, K. Dengler, T. Gerz, C. Schwarz, Prediction of dynamic pairwise wake vortex separations for approach and landing, AIAA Paper 2011-3037, 3rd AIAA Atmospheric Space Environments Conference, 27-30 June 2011, Honolulu, Hawaii, 15 pages, https://doi.org/10.2514/6.2011-3037.

[30] F. Holzäpfel, L. Strauss, C. Schwarz, Assessment of dynamic pairwise wake vortex separations for approach and landing at Vienna airport, AIAA Paper 2019-3178, AIAA Aviation Forum 2019, Dallas, TX, 17-21 June 2019, 22 pages, https://doi.org/10.2514/6.2019-3178.

[31] R. Sharman, C. Tebaldi, G. Wiener, J. Wolff, An integrated approach to mid- and upper-level turbulence forecasting, Weather Forecast. 21 (2006) 268–287, https://doi.org/10.1175/WAF924.1.

[32] D. Colson, H.A. Panofsky, An index of clear air turbulence, Q. J. R. Meteorol. Soc. 91 (390) (1965) 507–513, https://doi.org/10.1002/qj.49709139010.

[33] ICAO, Manual on Mode S Specific Services, Doc 9688, AN/952, 2nd edition, 2004.

[34] C.D. Donaldson, A.J. Bilanin, Vortex Wakes of Conventional Aircraft, NATO Rept. AG-204, Paris, 1975.

[35] D.P. Delisi, M.J. Pruis, F.Y. Wang, D.Y. Lai, Estimates of the Initial Vortex Separation Distance, b_0, of Commercial Aircraft from Pulsed Lidar Data, AIAA Paper 2013-0365, 51st AIAA Aerospace Sciences Meeting including the New Horizons Forum and Aerospace Exposition, 07 - 10 January 2013, Grapevine, Texas, 2013, 10 pages.

[36] Eurocontrol, FAA, Technical Report to Support the Safety Case for the Re-Categorization of ICAO Wake Turbulence Standards, 2011, 117 pages.

[37] BADA, User Manual for the Base of Aircraft Data (BADA) Revision 3.11, EEC Technical/Scientific Report No. 13/04/16-01, EUROCONTROL, May 2013, 109 pages, http://upcommons.upc.edu/bitstream/handle/2099.1/24342/AnnexI.pdf?sequence=2. (Accessed 29 June 2020).

[38] F. Holzäpfel, Analysis of potential wake vortex encounters at a major European airport, Aircr. Eng. Aerosp. Technol. 89 (5) (2017) 634–643, https://doi.org/10.1108/AEAT-01-2017-0043.

[39] F. Holzäpfel, R.E. Robins, Probabilistic two-phase aircraft wake-vortex model: application and assessment, J. Aircr. 41 (2004) 1117–1126, https://doi.org/10.2514/1.2280.

[40] F. Holzäpfel, Probabilistic two-phase aircraft wake-vortex model: further development and assessment, J. Aircr. 43 (2006) 700–708, https://doi.org/10.2514/1.16798.

[41] K.-U. Hahn, C. Schwarz, H. Friehmelt, A simplified hazard area prediction (SHAPe) model for wake vortex encounter avoidance, in: 24th International Congress of Aeronautical Sciences, 24th International Congress of Aeronautical Sciences Proceedings, Yokohama (Japan), 29 August - 3 September 2004, ICAS, 2004.

[42] C.W. Schwarz, K.-U. Hahn, Full-flight simulator study for wake vortex hazard area investigation, Aerosp. Sci. Technol. 10 (2006) 136–143, https://doi.org/10.1016/j.ast.2005.09.005.

[43] C.W. Schwarz, K.-U. Hahn, D. Fischenberg, Wake encounter severity assessment based on validated aerodynamic interaction models, in: AIAA ASE Conference, 2010.

[44] S. Körner, F. Holzäpfel, Assessment of the wake-vortex encounter probability on final approach based on lidar measurements, J. Aircr. 56 (2019) 1250–1258, https://doi.org/10.2514/1.C035252.

[45] Rules of the Air, Annex 2 to the Convention on International Civil Aviation, 10th ed., vol. 10, ICAO, Chicago, IL, July 2005, https://www.icao.int/Meetings/anconf12/Document%20Archive/an02_cons%5B1%5D.pdf. (Accessed 29 June 2020).

[46] T. Gurke, H. Lafferton, The development of the wake vortex warning system for Frankfurt airport: theory and implementation, Air Traffic Control Q. 5 (1997) 3–29, https://doi.org/10.2514/atcq.5.1.3.

[47] F. Holzäpfel, A. Stephan, G. Rotshteyn, S. Körner, N. Wildmann, L. Oswald, T. Gerz, G. Borek, A. Floh, C. Kern, M. Kerschbaum, R. Nossal, J. Schwarzenbacher, M. Stieber, M. Strobel, L. Strauss, C. Weiß, S. Kauczok, C. Schiefer, H. Czekala, G. Maschwitz, I. Smalikho, Mitigating Wake Turbulence Risk During Final Approach via Plate Lines, AIAA Paper 2020-2835, AIAA Aviation Forum 2020, Virtual Event, June 2020, 24 pages, https://doi.org/10.2514/6.2020-2835.

[48] F. Holzäpfel, J. Kladetzke, Assessment of wake vortex encounter probabilities for crosswind departure scenarios, J. Aircr. 48 (2011) 812–822, https://doi.org/10.2514/1.C000236.

[49] S. Kauertz, F. Holzäpfel, J. Kladetzke, Wake vortex encounter risk assessment for crosswind departures, J. Aircr. 49 (2012) 281–291, https://doi.org/10.2514/1.C031522.